Received 28 April 2009
Revised 1 August 2009
Accepted 10 September 2009

Numerical study of blood flow through different double bell-shaped stenosed coronary artery during the progression of the disease, atherosclerosis

D.K. Mandal
Department of Basic Science and Humanities, College of Engineering & Management, Kolaghat, India
N.K. Manna
Department of Mechanical Engineering, Jadavpur University, Kolkata, India, and
S. Chakrabarti
Department of Mechanical Engineering, Bengal Engineering and Science University, Shibpur, Howrah, India

Abstract

Purpose – This paper aims to perform numerical simulations through different shaped double stenoses in a vascular tube for a better understanding of arterial blood flow patterns, and their possible role during the progression of atherosclerosis. The dynamics of flow features have been studied by wall pressure, streamline contour and wall shear stress distributions for all models.
Design/methodology/approach – A finite volume method has been employed to solve the governing equations for the two-dimensional, steady, laminar flow of an incompressible and Newtonian fluid.
Findings – The paper finds that impact of pressure drop, reattachment length and peak wall shear stress at each restriction primarily depends upon percentage of restriction, if restriction spacing is sufficient. The quantum of impact of pressure drop, reattachment length and peak wall shear stress is much effected for smaller restriction spacing. If recirculating bubble of first restriction merges with the recirculating bubble formed behind the second restriction in this smaller restriction spacing. The similar effect of smaller restriction spacing is observed, if Reynolds number increases also.
Originality/value – The effect of different shaped stenoses, restriction spacing and Reynolds number on the flow characteristics has been investigated and the role of all the flow characteristics on the progression of the disease, atherosclerosis, is discussed.
Keywords Blood, Flow, Circulatory system, Cardiovascular disease, Shearing
Paper type Research paper

Nomenclature

A	Area at any section, [m^2]
D	Dia. of the artery [m]
h_f	Depth of the restriction [m]
L_i	Inlet length (i.e. length between inlet section and restriction-1) [m]
L_{ex}	Exit length (i.e. length between restriction-2 and exit section) [m]
Lr	Reattachment length [m]
Ls	Stricture length or length of stenosis [m]
P or p	Static pressure [N m^{-2}]
Pw	Wall pressure [N m^{-2}]
PR	Percentage of restriction or Percent stenosis = $2h_f/D \times 100\%$
R	Restriction

International Journal of Numerical Methods for Heat & Fluid Flow
Vol. 20 No. 6, 2010
pp. 670-698

0961-5539
DOI 10.1108/09615531011056827

Re	Reynolds number
S	Restriction spacing [m]
u_r	Velocity in r-direction [ms^{-1}]
u_z	Velocity in z-direction [ms^{-1}]
U	Average velocity in z-direction at inlet [ms^{-1}]
r, z	Cylindrical co-ordinates
ρ	Density [kg m^{-3}]
μ	Dynamic viscosity [kg m^{-1} s^{-1}]
τ_w	Wall shear stress [N m^{-2}]
τ_{wp}	Peak Wall shear stress [N m^{-2}]
Δp_w	Wall pressure drop at stenosis zone [N m^{-2}]

Subscripts

*	Dimensionless terms
1	Restriction-1
2	Restriction-2
1-1	Inlet
2-2	Exit

1. Introduction

Atherosclerosis is a progressive disease characterized by localized plaques that form within the artery wall. One of the fundamental causes of the plaque development is believed to be the abnormal enlargement of the intima by infiltration and accumulation of macromolecules such as lipoproteins, and the associated cellular and synthetic reactions. As the disease progresses, these plaques enlarge and, either directly or indirectly, lead to impairment of blood flow. This in turn can have serious consequences, such as blockage of the coronary arteries. It is also recognized that instead of a single stenosis, multiple stenoses may also develop in series in an arterial segment (Pincombe and Mazumdar, 1997; Moore, 1990). These constrictions in diseased vascular tube occur because the formation of the primary constriction produces recirculating flow at the downstream of the constriction depending on percent stenosis, stenosis length, flow Reynolds number, etc. This recirculating flow in time helps or assists particle accumulation and formation of a secondary constriction.

Both clinical reports and numerical simulations show that hemodynamics play an important role in the pathogenesis of atherosclerosis. It is widely believed that atherosclerosis development and progression are affected by many risk factors, such as static pressure, wall shear stress, blood viscosity, flow velocity, etc. The hemodynamic behavior of the blood flow in arterial stenoses bears some important aspects for medical applications.

The hemodynamical characteristics of flow through stenoses have been continually investigated numerically and experimentally for single as well as multiple restrictions. For single restriction flow, one of the numerical studies has been done by Cheng *et al.* (1972, 1974) to study numerically the growth of the vortex and local pressure variation considering rectangular shaped axisymmetrical restriction. Seeley and Young (1976), Solzbach *et al.* (1987), Liepsch *et al.* (1992) and Mandal and Chakrabarti (2007) have carried out the study to investigate the influence of geometric characteristics on flow pattern and pressure drop across rectangular shaped stenosis.

Mates *et al.* (1978) have studied the effect of axisymmetric and asymmetric (about the centre of the artery) trapezoidal shaped stenosis on flow characteristics. Ojha *et al.* (1989), Chahed *et al.* (1991), Lee and Xu (2002), Varghese and Frankel (2003), Jung *et al.* (2004) and Toufique Hasan and Das (2008) have considered axisymmetric trapezoidal shaped stenosis, of which the inlet shape and the outlet shape of stenosis are different.

The flow behavior through an artery with axisymmetric single bell-shaped stenosis has been studied by Lee and Fung (1970), Siouffi *et al.* (1998), Pontrelli (2001), Liao *et al.*

(2004), Misra and Shit (2006) and Mandal and Chakrabarti (2008). Numerical simulations by using single cosine shaped axisymmetric stenotic models have been carried out by Young and Tsai (1973a, b), Deshpande *et al.* (1976), Ahmed and Giddens (1983a, b), Tu *et al.* (1992), Tu and Deville (1996), Zendehbudi and Moayeri (1999), Varghese and Frankel (2003) and Liu *et al.* (2004) to investigate the distributions of pressure, wall shear stress and streamlines. A numerical and experimental investigation of transitional pulsatile flow in a circular shaped stenosed channel has been carried by Beratlis *et al.* (2005). Influence of rheology models for transient laminar axisymmetric flow through a tube with a cosine shaped stenosis is investigated by Buchanan *et al.* (2000). Mallinger and Drikakis (2002) have investigated the instabilities in pulsatile flow through a three-dimensional axisymmetric contour shaped stenosis with 75 percent reduction in the cross-sectional area. Neofytou and Drikakis (2003) have investigated the effect of non-Newtonian modeling on the unsteady periodic flow through an arc shaped stenosed 2D channel using different blood constitutive models. Mittal *et al.* (2003) have considered a simple model for studying blood flow through a one-sided semicircular constricted artery for the Reynolds numbers from 750 to 2,000 and a fixed pulsation frequency of 0.024. Their results showed a number of features that have been observed in previous experiments carried out in more realistic configurations. Sherwin and Blackburn (2005) have studied the three-dimensional instabilities and transition to turbulence of steady flow, steady flow plus an oscillatory component, and an idealized vascular pulsatile flow in a tube with a smooth axisymmetric sinusoidal constriction. Ramaswamy *et al.* (2004, 2006) have studied the effect of arterial motion of the human LAD coronary artery segment on the unsteady fluid dynamics with the morphologically realistic geometry of the segment reconstructed from intravascular ultrasound (IVUS) images fused with bi-plane angiographic images before and after angioplasty. The effect of non-Newtonian behavior of blood on pulsatile flows in stenotic arteries is investigated by Amornsamankul *et al.* (2006). The pulsatile flow of blood through mild axisymmetric contour shaped stenosed artery is studied by Sankar and Lee (2009). They have discussed pressure drop, wall shear stress, velocity, flow considering blood as a Newtonian fluid. A detail numerical study of the effects of variable blood viscosity on the flow field through an overlapping constriction has been carried out by Layek *et al.* (2009). Griffith *et al.* (2008, 2009) have considered a simplified model of arterial stenosis to show the effect of steady and pulsatile both inlet flow through a circular tube with an axisymmetric semicircular blockage of varying size numerically and experimentally.

For multiple restrictions, Solzbach *et al.* (1987) have investigated experimentally the influence of stenosis geometry, such as percentage lumen area reduction, length, exit angle and eccentric shape on the fluid dynamics of the post stenosis flow considering rectangular shaped restriction. Dreumel and Kuiken (1989) have studied numerically and experimentally the flow past through trapezoidal shaped double constrictions. Liepsch *et al.* (1992) have studied experimentally the influence of stenotic geometry under steady flow condition in four models of cylindrical stenosis with rectangular cross section. Tandom *et al.* (1993) have made an attempt to analyze the characteristics of the blood flow through an artery suffering with axisymmetric double stenoses in series. The stenoses are cosine shaped and identical with having each percentage of restriction of 20 percent. The stricture length (Ls*) of each restrictions is 1.0 and the restriction spacing (S*) between two restrictions is 1.25. The steady laminar flow fields in the neighborhoods of two consecutive Gaussian shaped restrictions have been studied by Lee (1994) for Reynolds number in the range of 5-200 considering the fixed percentage of restriction at the upstream restriction and different percentage of

restrictions at downstream restriction. Damodaran *et al.* (1996) have studied numerically the steady laminar flow through tubes with four constrictions. A numerical study of an unsteady laminar flow in a double contour shaped constricted 3D vessel has been carried out by Rathish Kumar *et al.* (2002). In their study, they have considered Re in the range of 100-1,200, and the spacing between the constrictions as 1, 2, 3, 4 and ∞ for fixed constriction (50 percent each) and Strouhal's number of 0.0124. Further, Lee (2002) has studied numerically the effects of steady flow through double similar symmetrical bell-shaped identical constrictions with percentage of restrictions of 33.3, 50 and 66.67 percent in tube for the Reynolds number in the range of 5-400, where the dimensionless restriction spacing is fixed as 1.0. Lee (2005) has also studied the flow fields in the neighborhood of double constrictions in a circular cylindrical tube for dimensionless spacings of 1, 2, and 3 with 50 percent restriction each.

From this brief review, it has been noted that the researchers have considered different shapes at inlet and outlet of the single stenosis configuration in case of trapezoidal shaped stenosis only. So far, no attempt has been made to study the influence of asymmetric configurations of stenosis on the flow characteristics considering realistic geometry of either single or multiple restrictions. It is also evident that researchers have considered the influence of multiple restrictions on the flow keeping fixed stricture length of each restriction. Besides this, no one has considered such type of multiple stenoses, where first restriction's PR changes and PR of second restriction is fixed. In the present study, initially, we have considered two consecutive similar symmetrical (about the centre of bell) restrictions with 30 percent PR each. Then it is thought that the progression of first restriction changes its shape keeping no change in the shape of second restriction. Firstly, the shape of first restriction changes along its length downstream to the stenosis at same PR of 30 percent. Secondly, the shape of first restriction changes along its stricture length and percentage of restriction both. The effect of different shaped double stenoses on flow characteristics, for example, wall pressure drop, streamline contour and peak wall shear stress has been investigated, and comparisons with single restriction ($S = \infty$) have been presented for a fixed Reynolds number of 100 only. Apart from this study, the effect of restriction spacing and Reynolds number on the above flow parameters has been highlighted. This type of fluid flow study through wavy boundaries has also of great interest to engineers and researchers because of the importance it plays in phenomena such as: the generation of wind waves on water; the stability of a liquid film in contact with a gas stream; the transpiration cooling of reentry vehicles and rocket boosters; film vaporization in combustion; and fluid flow in pipes with fittings.

2. Mathematical formulation

2.1 Governing equations

A schematic diagram of the computational domain is illustrated in Figure 1. It shows the computational domain with Gaussian shaped restrictions. This bell-shaped stenosis geometry is modeled mathematically as $r = 0.5 - h_f \exp\left((-4m^2z^2)/L_s^2\right)$ (Misra and Shit, 2006), where m is a parametric constant. The flow under consideration has been assumed to be steady, two-dimensional, laminar and axisymmetric. Since the development of arteriosclerosis in arteries reduce the elastic property of the arterial wall, therefore, in our study, the vessel wall has been considered as rigid tube (Liu *et al.*, 2004). It is established that for the diameter of artery $\geq$0.2 mm, shear rate becomes very high which leads for the consideration of blood as a Newtonian fluid for coronary artery, whose diameter is approximately 0.3 cm[1]. Therefore, in our study, the fluid, that is, blood is considered to be

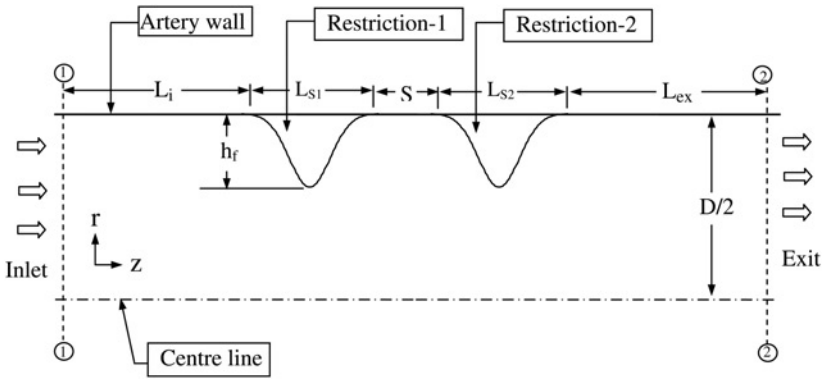

Figure 1.
Computational domain

Newtonian and incompressible. The flow of blood in the blood vessels, like the flow of liquids in narrow rigid tubes, is normally considered laminar (Ganong, 2001). From the literatures of Andersson *et al.* (2000) and Back and Banerjee (2000), it is established that physiological flow range of Reynolds number is 100-400 for main coronary artery of human being in the laminar zone. Bertolotti *et al.* (2001) have also mentioned that the critical Reynolds number of the flow of blood through coronary artery is in between 300 and 400, above which the flow becomes transitional and turbulent at 75 percent stenosed condition. Therefore, the consideration of flow as laminar at our considered Reynolds number up to 400 seems to be reasonable.

The following dimensionless variables are defined to obtain the governing conservation equations in the non-dimensional form:

Lengths: $r^* = r/D$, $z^* = z/D$, $L_i^* = L_i/D$, $L_{ex}^* = L_{ex}/D$, $L_{S1}^* = L_{s1}/D$, $L_{S2}^* = L_{s2}/D$, $L_r^* = L_r/D$, $h_f^* = h_f/D$, $S^* = S/D$.
Velocities: $u_r^* = u_r/U$, $u_z^* = u_z/U$.
Pressure: $p^* = p/\rho U^2$.

With the help of these variables, the mass and momentum conservation equations are written as follows:

$$\frac{\partial}{r^* \partial r^*}(r^* u_r^*) + \frac{\partial}{\partial z^*}(u_z^*) = 0 \tag{1}$$

$$\frac{\partial(r^* u_r^* u_r^*)}{r^* \partial r^*} + \frac{\partial(u_z^* u_r^*)}{\partial z^*} = -\frac{\partial p^*}{\partial r^*} + \frac{1}{Re}\left(\frac{\partial}{\partial r^*}\left(\frac{\partial(r^* u_r^*)}{r^* \partial r^*}\right) + \frac{\partial^2 u_r^*}{\partial z^{*}2}\right) \tag{2}$$

$$\frac{\partial(r^* u_r^* u_z^*)}{r^* \partial r^*} + \frac{\partial(u_z^* u_z^*)}{\partial z^*} = -\frac{\partial p^*}{\partial z^*} + \frac{1}{Re}\left(\frac{\partial}{r^* \partial r^*}\left(r^* \frac{\partial u_z^*}{\partial r^*}\right) + \frac{\partial^2 u_z^*}{\partial z^{*2}}\right) \tag{3}$$

where the flow Reynolds number, $Re = \rho UD/\mu$.

2.2. Boundary conditions
Four different types of boundary conditions have been applied to the present problem. They are as follows,

(1) *At the walls*: No slip condition, i.e., $u_r^* = 0,\ u_z^* = 0$.

(2) *At the inlet*: Axial velocity has been specified and the transverse velocity has been set to zero, i.e., $u_z^* = specified,\ u_r^* = 0$. Fully developed flow condition has been specified at the inlet, i.e., $u_z^* = 2.0[1 - (2_r^*)^2]$.

(3) *At the exit*: Fully developed condition has been assumed and hence gradients have been set to zero, i.e., $\partial u_z^*/\partial_z^* = 0,\ u_r^* = 0$.

(4) *At the line of symmetry*: The normal gradient of the axial velocity and the transverse velocity have been set to zero, i.e., $\partial u_z^*/\partial_r^* = 0,\ u_r^* = 0$.

2.3 Numerical procedure

The governing equations (1)-(3) have been solved numerically by an in-house CFD code developed using integral approach of the finite volume method on a non-uniform staggered grid following SIMPLER algorithm (Patankar, 1980). The third-order upwind scheme has been used for advective part. The discretized equations have been solved using tri-diagonal matrix algorithm with alternate direction implicit scheme. The convergence of the iterative scheme has been achieved when the normalized residuals for mass and momentum equations summed over the entire calculation domain will fall below 10^{-7}.

In the computation, flow has been considered fully developed at inlet and exit, and therefore, the non-dimensional total length of computational domain has been chosen to be 200 and the inlet length has been chosen to be 50. After grid independence test, finally the numerical mesh comprised of 449 $\times$ 65 grid nodes in z and r direction has been considered in the present work.

2.4 Validation of computational results

To check the validity of the numerical results, numerical computations to steady flow through a cosine shaped single stenosis of 56 percent area reduction are performed for different values of Reynolds number. This study has been carried out for the stricture length of 4.0, percentage of restriction of 33.33 percent and the non-dimensional length of the computational domain of 16. This geometry has also been used by Young and Tsai (1973a) in their experimental studies, Zendehbudi and Moayeri (1999) and Lee (2002) in their numerical solutions, therefore, comparisons of dimensionless pressure drop, and separating and reattachment curves can be made with previous theoretical and experimental results.

The variations of dimensionless pressure drop (Δp^*) with Reynolds number are compared with experimental values of Young and Tsai, numerical values of Zendehbudi and Moayeri and Lee, shown in Figure 2. This shows a good agreement with other work.

The separation-reattachment curves from different studies are shown in Figure 3. There is a good agreement between present result and numerical results of Zendehbudi and Moayeri (1999). Apparently, the large discrepancy with experimental results of Young and Tsai (1973a) has been observed, since the reattachment length is difficult to ascertain experimentally.

In order to validate axial velocity profiles, numerical study has been carried out for the Ls* of 1.25, percentage of restriction of 50 percent and for the Re of 200 through cosine shaped single restriction, which has also been computed by Tu *et al.* (1992) and Deshpande *et al.* (1976). Figure 4 gives axial velocity profiles at different axial locations for Re of 200. The locations are chosen such that comparisons can be made with the computational results of Tu *et al.* The velocity profile is parabolic at the upstream

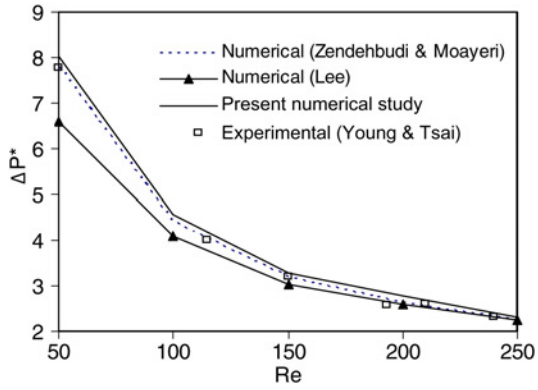

Figure 2.
Variations of dimensionless pressure drop

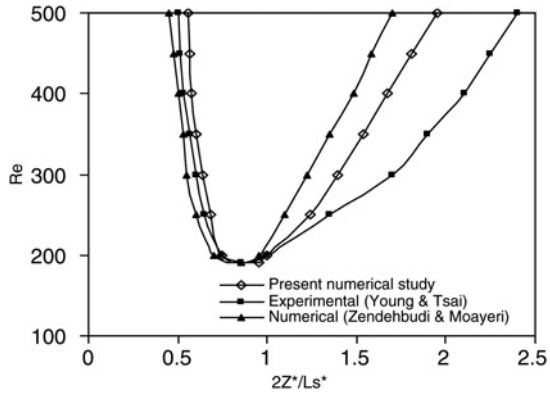

Figure 3.
Separation-reattachment curves

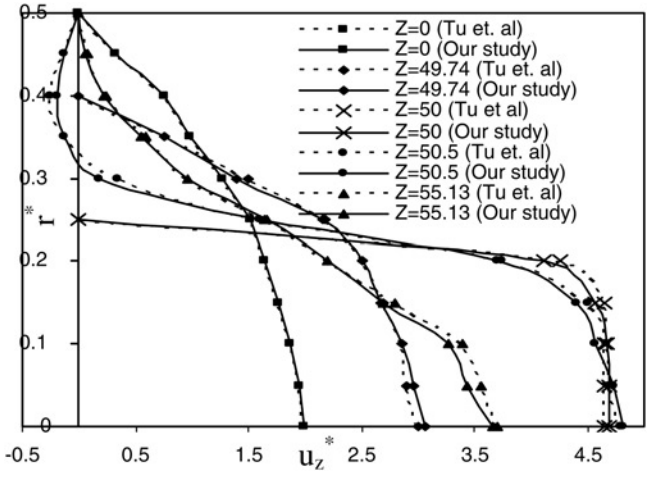

Figure 4.
Axial velocity profiles at different axial locations

section (Z* = 0.0), it then tends to flatten at the converging section (Z* = 49.74), it becomes blunter at the throat (Z* = 50.0), than at the entry. Slightly downstream from the throat ((Z* = 50.5), the velocity presents a reversal zone near the wall which disappears at Z* = 55.13. These velocity profiles match very well with those obtained by Tu *et al.* Since Tu *et al.* have shown good agreement with Despande *et al.* for these velocity profiles. This indicates that our computed results match very well for the velocity profiles presented by Tu *et al.* and Despande *et al.*

2.5 Problem formulation

It is difficult to say how the shape of stenosis takes place at the initiation and progression of the disease, atherosclerosis. The shape of stenosis does not obey any rule. The shape of stenosis may change in two directions. One is in the z direction, i.e., by increasing the length of stenosis, another is in the r direction, i.e., by increasing the percentage of restriction. In case of double stenoses, most of the researchers have varied the percentage of restriction of stenosis keeping stricture length same. It seems to be quite unnatural to think that the shape of stenosis increases in the z direction only. Instead, it is more reasonable to think that the shape should increase both in r and z directions. This idea has been considered in our problem formulation. In our study, we have considered two aspects of progression of stenosis shape, for one, downstream of the stenosis is the prone zone of aggravation and for other one, both the throat and downstream are the prone zone of aggravation of the stenosis.

The formulations of different shapes are shown in Figure 5 and the details of different shapes are presented in Table I. Initially we have considered a double stenoses

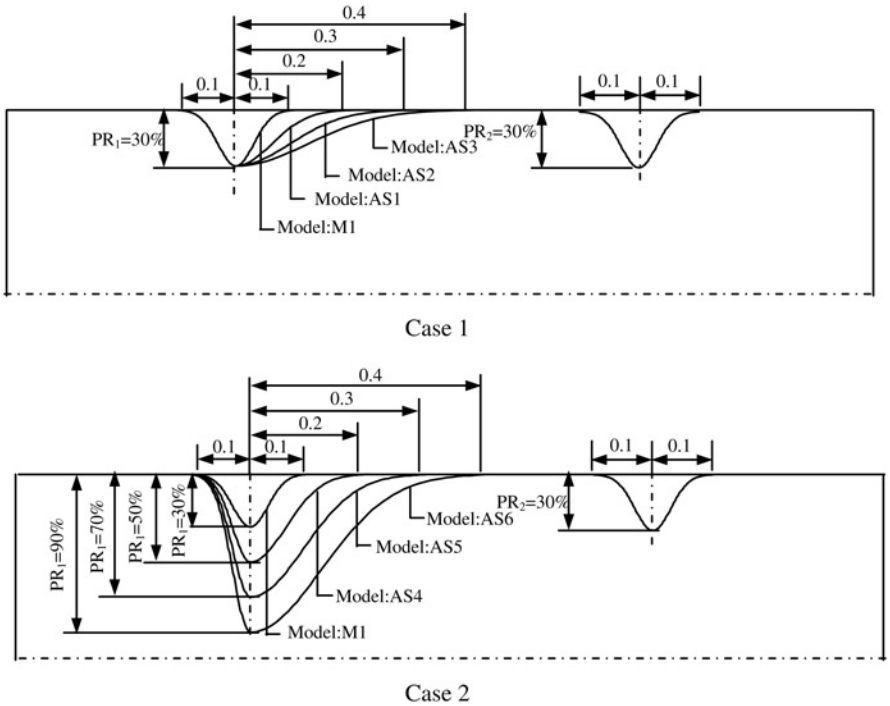

Figure 5.
Different shapes

like the model:M1, where both restrictions are similar symmetrical (about the center of restriction) having same stricture length of 0.2 and PR of 30 percent each. If the aggravation takes place only in the downstream of first stenosis of model:1, then the shape of first restriction of double stenoses changes from M1 to AS1, AS1 to AS2 and AS2 to AS3 sequentially. For all models, the shape of restriction-2 remains same like the model:M1. All these considerations have been grouped in case 1. The case-2 indicates the aggravation of stenosis mainly at the throat and downstream zones of first restriction of model:M1. Therefore, the shape of first restriction of multi-stenoses changes from M1 to AS4, AS4 to AS5, and AS5 to AS6. Here also, the shape of second restrictions remains same as model:M1.

3. Results and discussion

Numerical simulations have been carried out to model the steady flow of blood through a coronary artery with double bell-shaped stenoses. During numerical investigation; firstly, the effect of different shaped double stenoses (for case-1 and case-2) on flow characteristics, for example, wall pressure drop, streamline contour and peak wall shear stress, and comparisons with single restriction ($S^* = \infty$); secondly, the effect of restriction spacing, and lastly the effect of Reynolds number for some specific shaped stenoses on the above flow parameters have been carried out.

3.1 Effect of shape of stenoses (for case-1 and case-2)

In this subsection, the effect of different shaped double stenoses like case-1 and case-2 on wall pressure, streamline contour and wall shear stress has been investigated and comparisons have been made with single restriction. For all our considered double stenoses, the shape of restriction-2 remains fixed. In case-1, the aggravation of the first stenosis takes place in the downstream only keeping percentage of restriction same. For case-2, both the stricture length and percentage of restriction of first restriction increase due to aggravation of disease. The restriction spacing between two restrictions has been considered as 4.0 for model:M1.

The parameters during the study are identified as:

- Reynolds number = 100;
- percentage of restriction = 30, 50, 70 and 90 percent;
- restriction spacing = 4.0, 3.9, 3.8 and 3.7; and
- stricture length = 0.2, 0.3, 0.4, 0.5.

3.1.1 Variation of wall pressure. The variations of wall pressure have been shown in Figure 6 for Reynolds number of 100 for case-1. The general trend of the curves is noted

Model	Ls^*_1	PR_1 (%)	Ls^*_2	PR_2 (%)	Case
M1	0.2	30	0.2	30	Case-1
AS1	0.3	30			
AS2	0.4	30			
AS3	0.5	30			
M1	0.2	30	0.2	30	Case-2
AS4	0.3	50			
AS5	0.4	70			
AS6	0.5	90			

Table I.
Details of different shapes

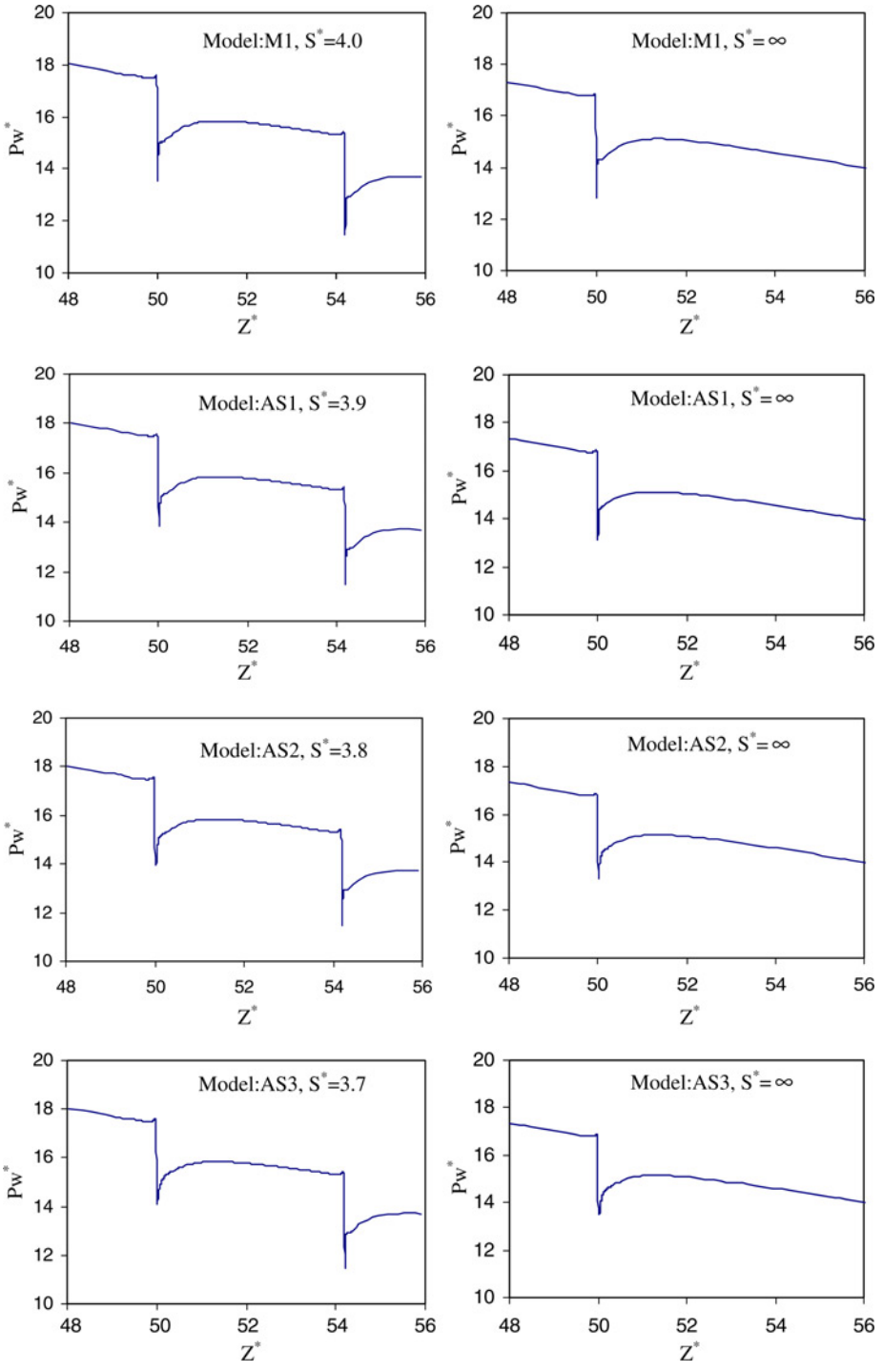

Figure 6.
Variations of wall pressure for Re = 100 for case-1

to be decreasing in nature from the inlet to the entry of first restriction. This may be attributed due to the friction throughout this length of tube. Then a slight upstream rise at the entry of restriction-1 has been noted due to stagnation effect of flow. At the first restriction zone, sharp pressure drop has been observed due to primarily viscous effect. After that, at the vicinity of the downstream of restriction-1, sharp pressure rise takes place due to higher diffusion. When the fluid reaches the vicinity of the upstream of second restriction, another pressure rise of higher magnitude has been observed. Then the pressure sharply decreases at the second restriction like the first restriction. Again a sharp pressure rise has been noted at the downstream of second restriction. From the figure, it is evident that the magnitude of the dimensionless pressure drop across the first restriction (ΔPw^*_1) decreases, when the model:M1 changes to AS1, AS2 and AS3, as stricture length of first restriction (Ls^*_1) increases and corresponding restriction spacing (S*) decreases. Magnitudes of ΔPw^*_1 for the said models are noted to be same like the case of single restriction ($S^* = \infty$). This is also shown in Figure 7. It indicates that the effect of different shape of first restriction on wall pressure remains same like the single restriction. It is also observed that there is no much impact of the automatically evolved changes in restriction spacing on the wall pressure drop in the first restriction. The probable reason behind the observation may be due to higher restriction spacing. The magnitude of non-dimensional pressure drop at restriction-2 (ΔPw^*_2) has been noted to be fixed for all the models, as stricture length and percentage of restriction of restriction-2 remains fixed. This is also shown in Figure 7. Therefore, it can be said that there is no impact of first restriction and restriction spacing on second restriction for the considered cases.

Figure 8 shows the variations of wall pressure for different models in case-2 for Reynolds number of 100. The trend remains same like the earlier observations made in case-1. Here, ΔPw^*_1 increases with the change of considered models from M1 to AS6 of case-2. In this case, the trend in the increase in stricture length (Ls^*_1) and decrease in restriction spacing (S*) has been kept same as case-1. In this type of aggravation, ΔPw^*_1 increases due to the high impact of restriction compared to the effect of stricture length and restriction spacing. The magnitude of ΔPw^*_1 is same with the pressure drop observed in case of single restriction for the models M1 and AS4 only. The magnitude of ΔPw^*_1 for the models AS5 and AS6 are greater than the magnitude

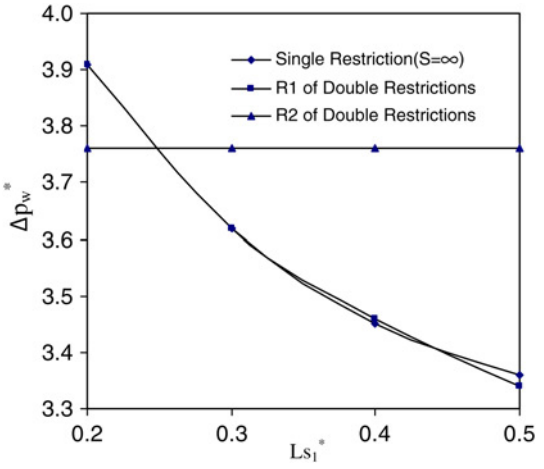

Figure 7.
Variations of wall pressure drop at stenosis zone for Re = 100 for case-1

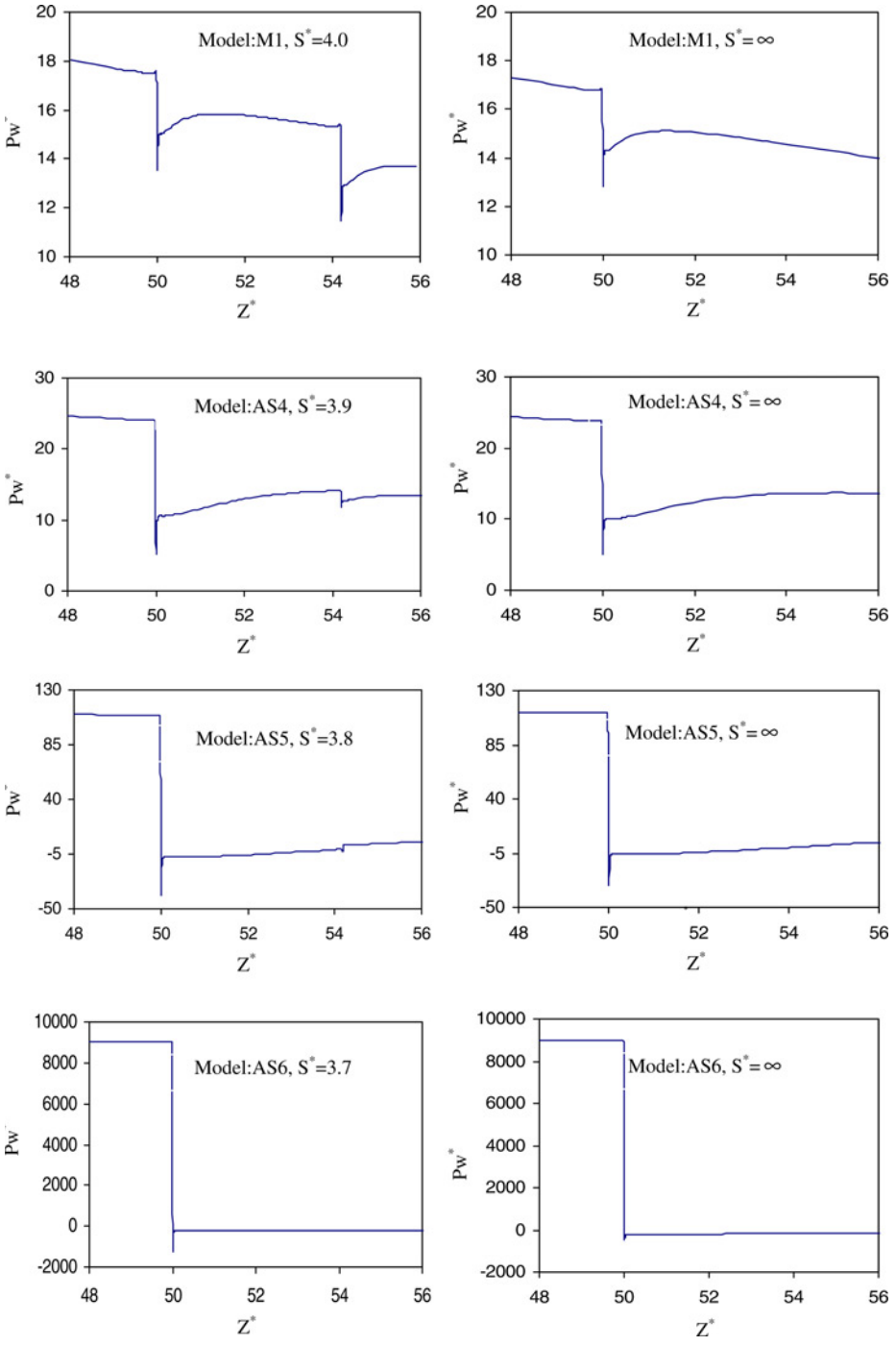

Figure 8.
Variations of wall pressure for Re = 100 for case-2

for single restriction. These happenings may be due to the higher impact of higher length of recirculation bubble at the downstream of first restriction due to higher PR_1. For this case-2, ΔPw^*_2 decreases with the changes of models from M1 to AS6, probably due to higher PR_1.

The atheromatous plaques appear in the regions of low pressure, where a suction action exerted on the surface endothelium which causes the layer to be selectively separated from adjacent tissue. This tearing action is thought to cause of damaging the endothelium and adjacent wall layers, with subsequent thickening of the intima and eventual plaque development. Therefore, if the aggravation of stenosis takes place like case-1, the chance of tearing and collapsing of artery at restriction-1 (R_1) decreases, whereas the physiological impact of wall pressure at restriction-2 (R_2) remains same. For case-2, the physiological impact of wall pressure drop at R_1 on progression of the disease increases, but this impact decreases at R_2.

3.1.2 Variation of streamlines contour. Figure 9 shows the streamline contours for case-1. From the streamlines, it is noted that separation phenomenon occurs downstream to the throat section and it reattaches at some distal location at $Re = 100$ for all the restrictions. Variations of reattachment length for all the considered models are shown in Figure 10. It is noted from Figures 9 and 10, that the length of recirculation zone for first restriction (Lr^*_1) decreases with the increase of stricture length (Ls^*_1), when the model changes from M1 to AS3. The magnitude of Lr^*_1 has been noted to be same with the reattachment length formed in case of single stenosis. This indicates that there is no impact of restriction spacing on recirculation length, may be due to higher restriction spacing. The magnitude of reattachment length of second restriction (Lr^*_2) does not change in these models of case-1.

The variations of streamline contour have been shown in Figure 11 for Reynolds number of 100 in case-2. In this case, when the model changes from M1 to AS6, Lr^*_1 increases in spite of opposite impact of stricture length on the length of recirculation zone. This indicates high impact of PR on recirculation length compared to stricture length. It is noted from Figure 11 that the magnitudes of Lr^*_1 are same with the recirculation length formed with single restriction for the model M1 and AS4 due to higher restriction spacing. In case of models of AS5 and AS6, the inner zone between two restrictions is fully filled up by recirculation bubble. Moreover, it is noted that the recirculating eddy between the two constrictions spreads beyond the second restriction and merges with the eddy that formed behind the second restriction. The total length of recirculation zone of double stenoses (model:AS5 and AS6) is more compared to recirculation length formed in case of single restriction.

Since the recirculation zone is the cause of stagnation of blood stream and allows platelets and fibrin to form a mesh at the inner wall in this zone by trapping lipid particles to form atheromatous plaque, therefore the plaque deposition zone at R_1 decreases and the plaque deposition zone at R_2 remains same in case-1. For case-2, plaque deposition chance at R_1 increases. When model changes from M1 to AS4, the plaque deposition zone increases at R_2; whereas, for the models of AS5 and AS6, these zones are noted to be increasing with increase in PR considering both impact of R_1 and R_2.

3.1.3 Variation of wall shear stress. The non-dimensional wall shear stress at any position is computed with the help of the following expression:

$$\tau^*_w = \frac{\tau_w}{\tau_{wref}}$$

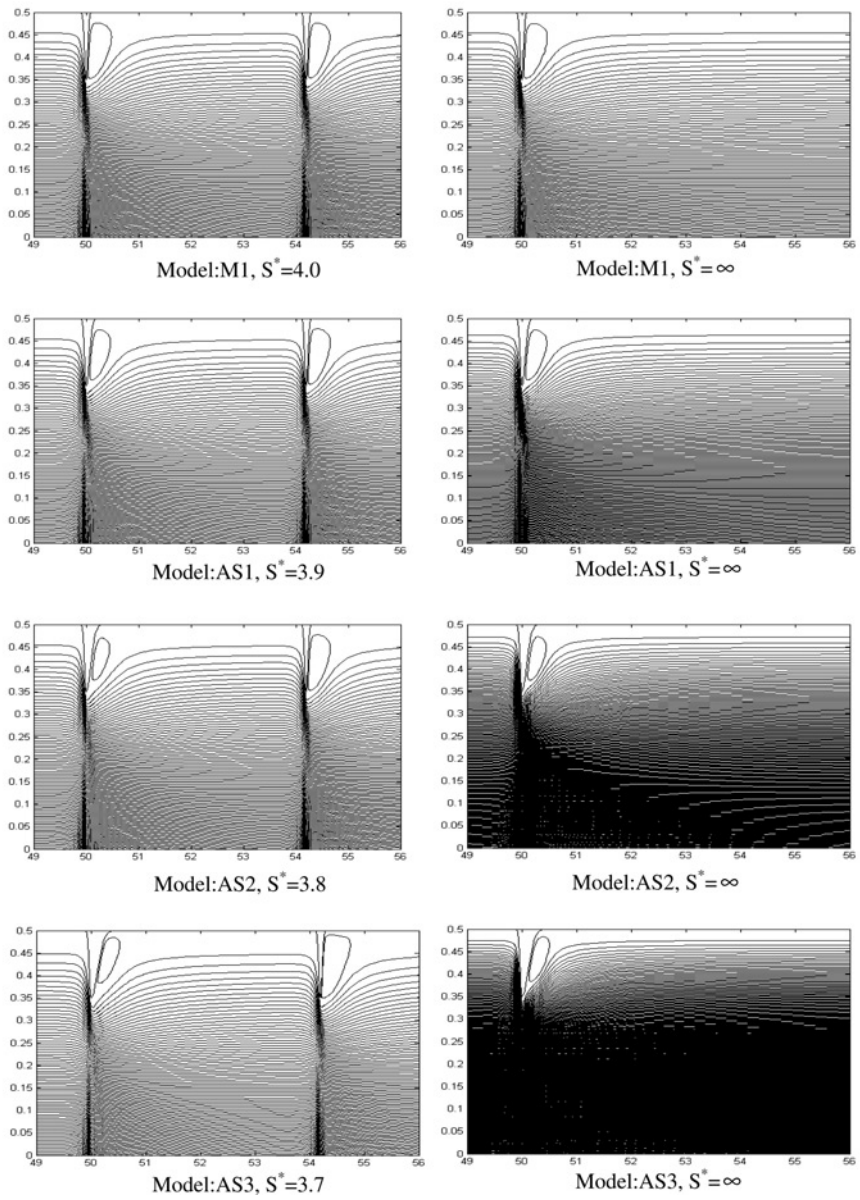

Figure 9.
Contours plotting for Re = 100 for case-1

where τ_w is wall shear stress and τ_{wref} is the reference wall shear stress, which is considered as the wall shear stress far away from the stenosis.

The general trend of the curves of wall shear stress for case-1 (Figure 12) shows that rise of wall shear stress occurs at the restriction zone due to high velocity gradient and then it attains negative wall shear stress at the downstream of restriction due to adverse pressure gradient for all restrictions. The variations of peak wall shear stress for the case

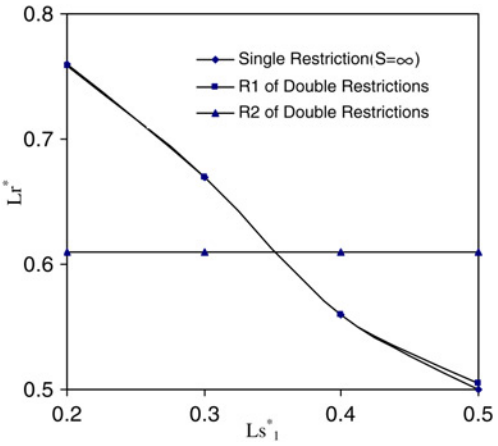

Figure 10.
Variations of reattachment length for Re = 100 for case-1

have been shown in Figure 13. From the study, it is noted that the magnitude of non-dimensional peak wall shear stress for first restriction (τ_{wp}*$_1$) decreases, when model changes from M1 to AS3. This happens probably due to decrease in stricture length (Ls*$_1$). The magnitude of τ_{wp}*$_1$ is observed to be same with the magnitude of peak wall shear stress developed for single restriction. Therefore, the impact of restriction spacing on peak wall shear stress developed in R_1 is also negligible due to higher S*. The magnitude of τ_{wp}*$_2$ has been observed to be same for all models in this case. This indicates that there is no impact of restriction spacing on the peak wall shear stress at second restriction.

Figure 14 shows the variations of wall shear stress for Reynolds number of 100 for case-2. It is evident from the figure that the magnitude of τ_{wp}*$_1$ increases with increase in PR_1. This magnitude is more compared to the value of peak wall shear stress in case of single restriction for the models of AS4, AS5 and AS6. It may be due to higher PR of R_1 in comparison to PR of second restriction. The magnitude of τ_{wp}*$_2$ decreases in case-2 and finally attains negative value. This happens due to merging of recirculation eddy for models of AS5 and AS6 of the first restriction with the eddy formed behind the second restriction. Inset figure in case of model:AS6, shows the variation of wall shear stress at the second restriction (R_2), which could not been shown in the main figure due to higher magnitude of scale for τ_{wp}*.

It is known that high wall shear stress is considered to be a possible initiating factor in atherosclerosis. It damages the vessel wall and causes intimal thickening. Side by side, low wall shear stress in the separation region causes the mass transportation across the arterial wall. Therefore, the damaging chance of arterial wall due to peak wall shear stress at R_1 decreases in case-1. This chance of damage remains same at R_2. For case-2, the phenomenon of arterial wall damage due to peak wall shear stress at R_1 increases. This impact of peak wall shear stress on the phenomenon for second restriction decreases with the increase in percentage of restriction of first restriction. Finally at higher PR_1, the impact at low wall shear stress appears and chance of aggravation of the disease takes place accordingly.

3.2 Effect of restriction spacing (for model:M1 and model:AS4)

In this subsection, we have chosen two models. One is model:M1, the shape of two restrictions are similar symmetrical with PR of 30 percent each. Another model is AS4, the first restriction is asymmetrical with PR of 50 percent and the second restriction is

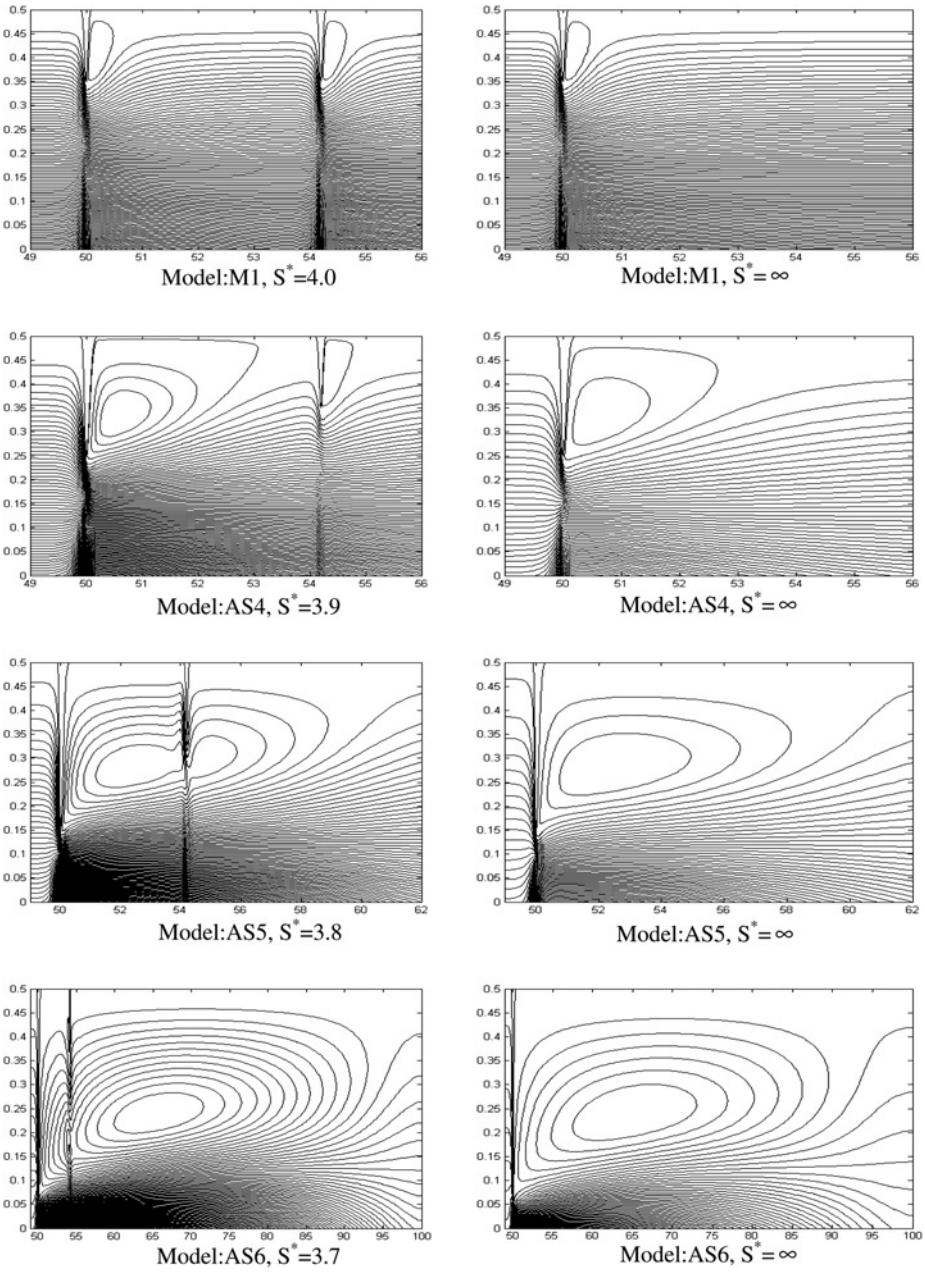

Figure 11.
Contours plotting for Re = 100 for case-2

symmetrical with 30 percent restriction like model:M1. Intentionally the stated two models have been considered to investigate the effect of restriction spacing on the flow characteristics for the cases, when for one, two restrictions are symmetric with same PR; and for other one, the upstream restriction is asymmetric with higher PR along

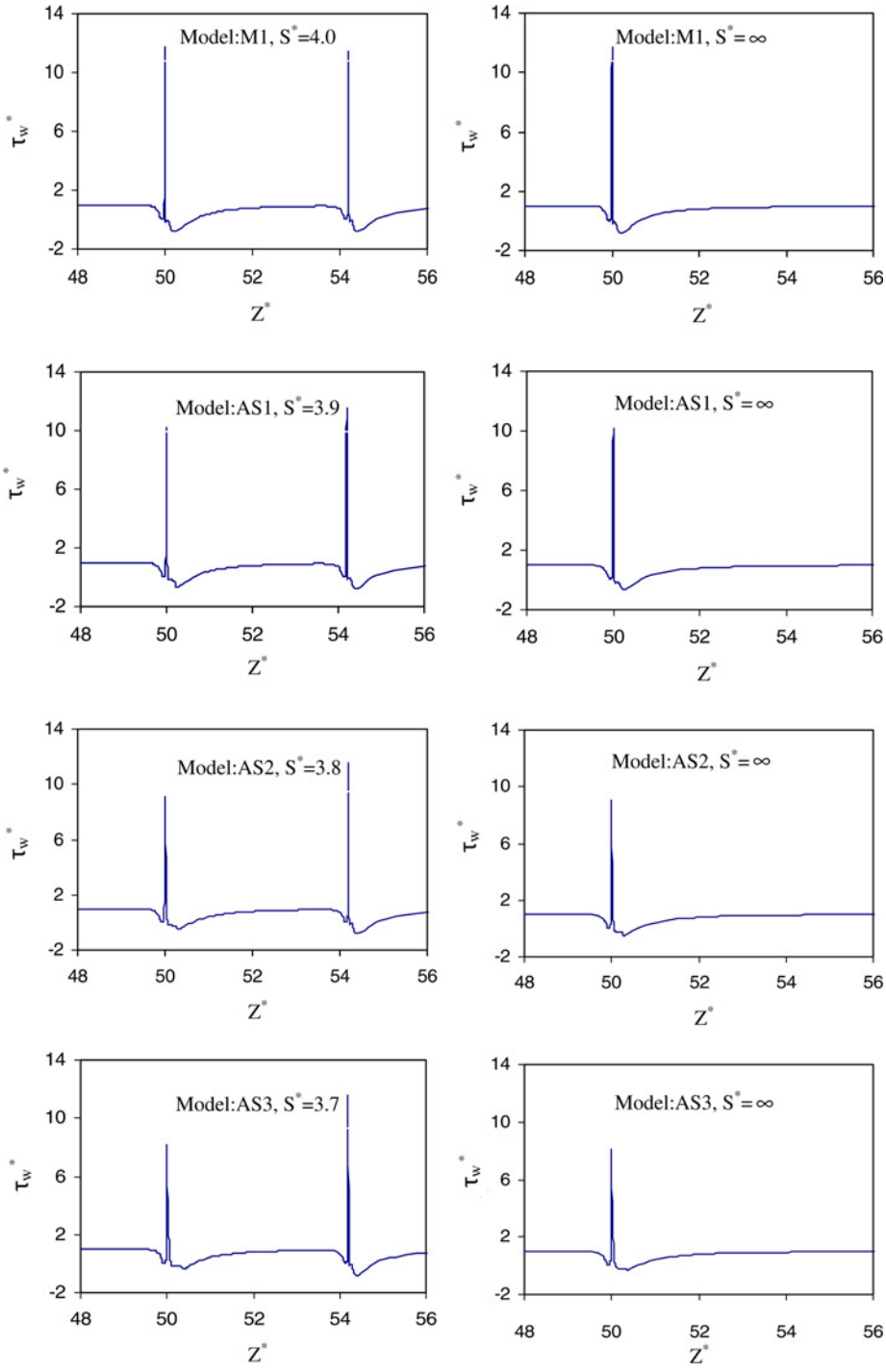

Figure 12.
Variations of wall shear stress for Re = 100 for case-1

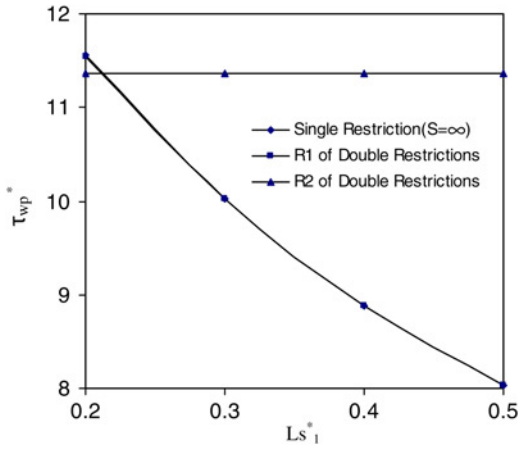

Figure 13.
Variations of peak wall shear stress for Re = 100 for case-1

with the same configurations of the downstream restriction as was considered for the earlier one. Since for the first model:M1, PR of upstream restriction is 30 percent; and for the second model:AS4, PR of upstream restriction is 50 percent, therefore, during numerical investigation, the restriction spacings for model:M1 have been considered to be 0.5, 1.0, 2.0 and 4.0, and restriction spacings for AS4, have been considered to be 2.9, 3.9, 4.9 and 5.9, respectively. Finally for both the cases, the effect of restriction spacing on wall pressure, streamline contour, and peak wall shear stress has been investigated for a typical value of Reynolds number of 100.

Figure 15 shows the variations of dimensionless wall pressure for both the models M1 and AS4 for the Reynolds number of 100. Corresponding wall pressure drops at the restriction zone for both the models M1 and AS4 have been presented in Figure 16. It is noted from Figures 15 and 16 that the major part of the pressure drop in the restricted tube has been observed across the first restriction for each model of M1 and AS4. The magnitude of the pressure drop across the first restriction has been noted to be same for the entire S* for model:M1. Similarly, in case of model:AS4, the magnitude of wall pressure drop across the first restriction for their considered S* remains same. Pressure drop in the second restriction increases with S* for each model. From Figure 16, comparing the curve of each model (R_2, model:M1; and R_2, model:AS4), it can be stated that the pressure drop at stenosis zone at R_2 is higher for the model:M1 than the model:AS4 in the common range of S*. This may happen due to higher PR_1 of model:AS4.

The variations of streamline contour for the above considered models have been shown in Figure 17. From the figure, it is observed that the size of recirculating bubble downstream to the first restriction is more compared to the second restriction for both considered models (M1 and AS4). In each model, it is noted that the magnitude of the dimensionless reattachment length downstream to the first restriction is same for the entire S* in case of respective model separately. The size of recirculating bubble for the second restriction does not change appreciably for each model. This may be due to large restriction spacing, as there is no merging of recirculating eddy from the first restriction behind the second restriction.

The variations of wall shear stress for the models M1 and AS4 have been shown in Figure 18, and the variations of peak wall shear stress for these models have been shown in Figure 19. From the study, it is noted that major rise in wall shear stress occurs in the first restriction for both the models. Its magnitude ($\tau_{wp}{}^*{}_1$) for each model

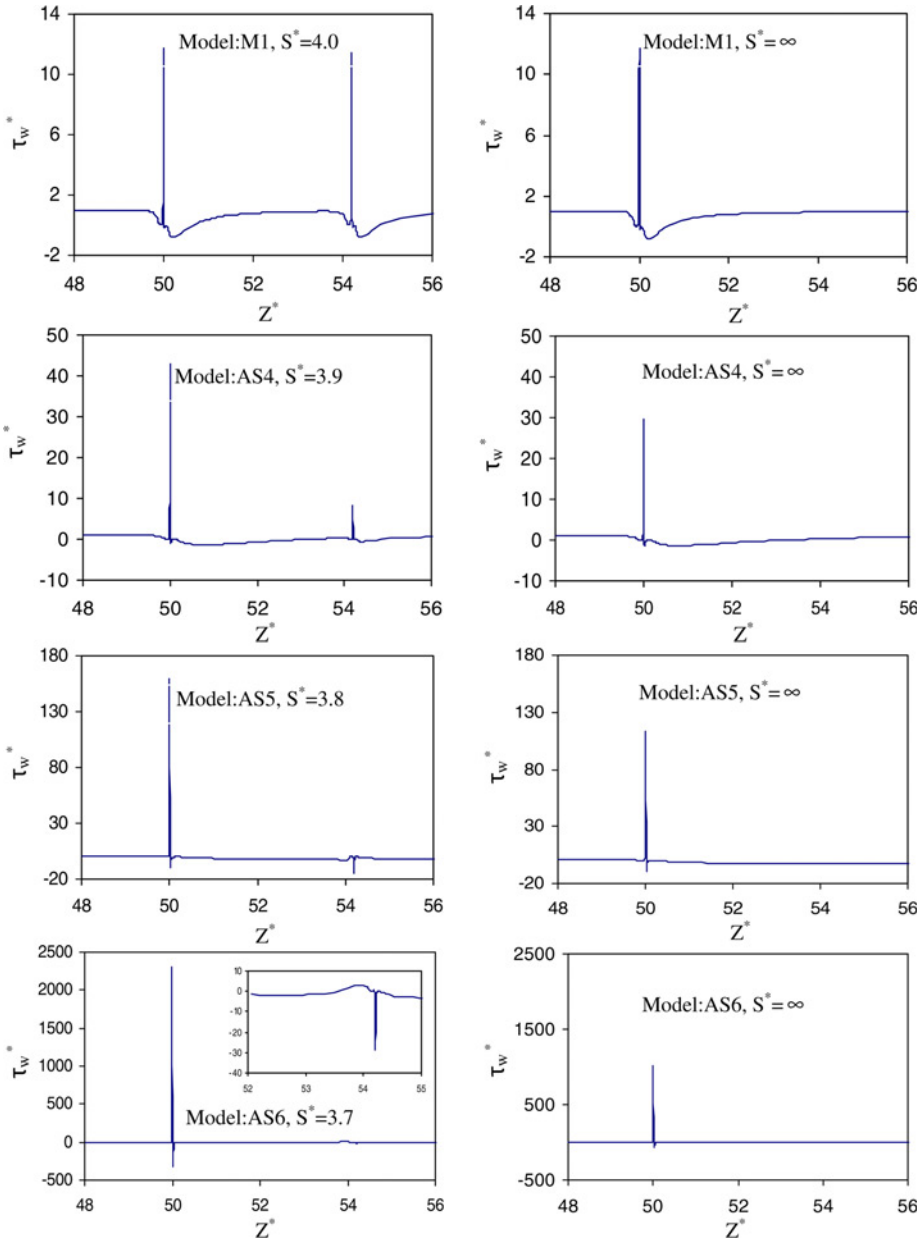

Figure 14.
Variations of wall shear stress for Re = 100 for case-2

is observed to be same for all the restriction spacing in the case of respective model. The magnitude $\tau_{wp}{}^{*}{}_{2}$ increases with restriction spacing for all the models (M1 and AS4). From Figure 19, it is noted that in case of second restriction for both the models in the common range of S*, the magnitude of peak wall shear stress in case of model:M1 is larger than that of the magnitudes of peak wall shear stress of model:AS4.

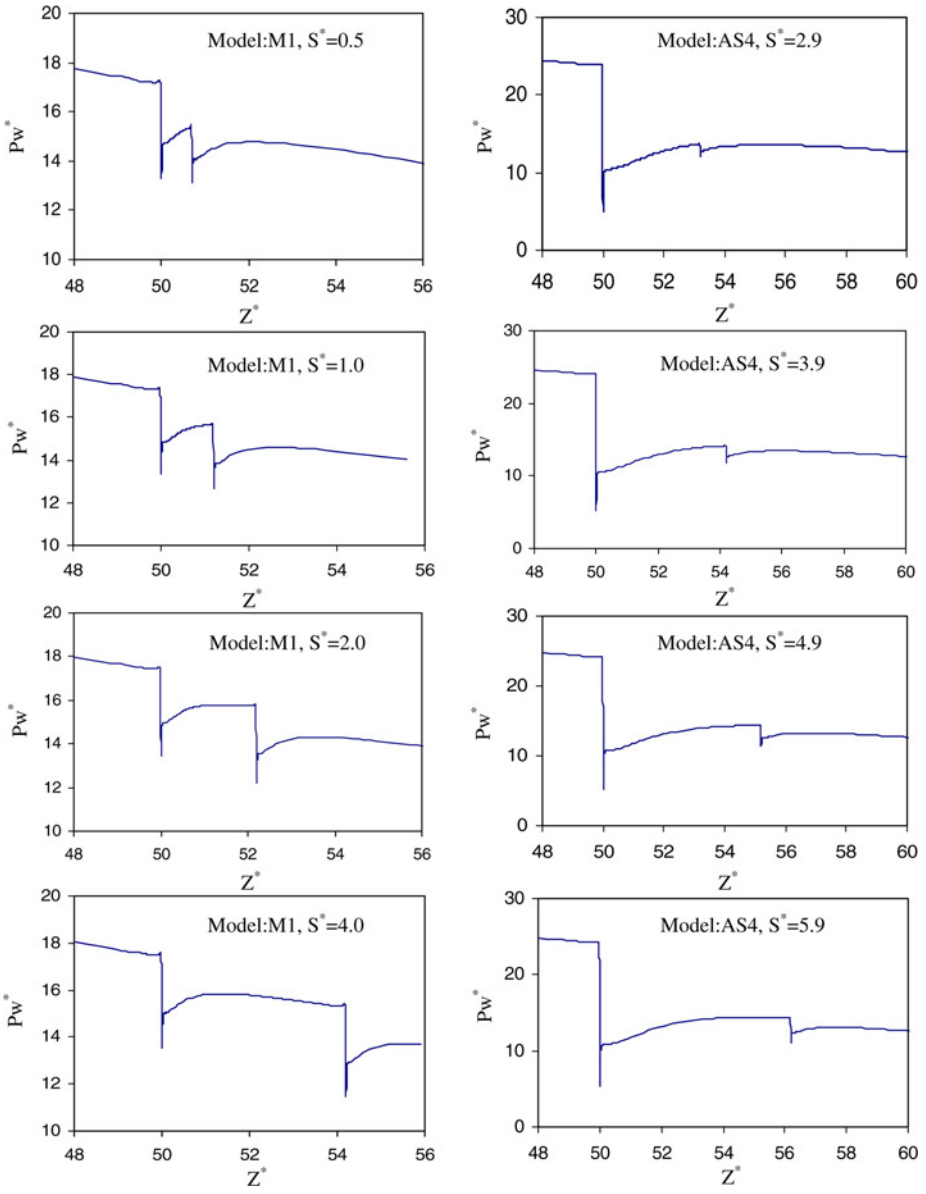

Figure 15.
Variations of wall pressure for Re = 100

Therefore, there is more chance of tearing action of artery wall due to higher wall pressure drop at the first restriction with respect to pressure drop at second restriction for all the considered restriction spacings. This chance of tearing action of the artery wall at the first restriction is noted to be same for all the restriction spacings in case of respective models separately. But the chance of tearing action increases with S* at second restriction for all considered models. However, more chance of tearing action due to pressure drop at second restriction is noted to occur in case of M1 in the range of

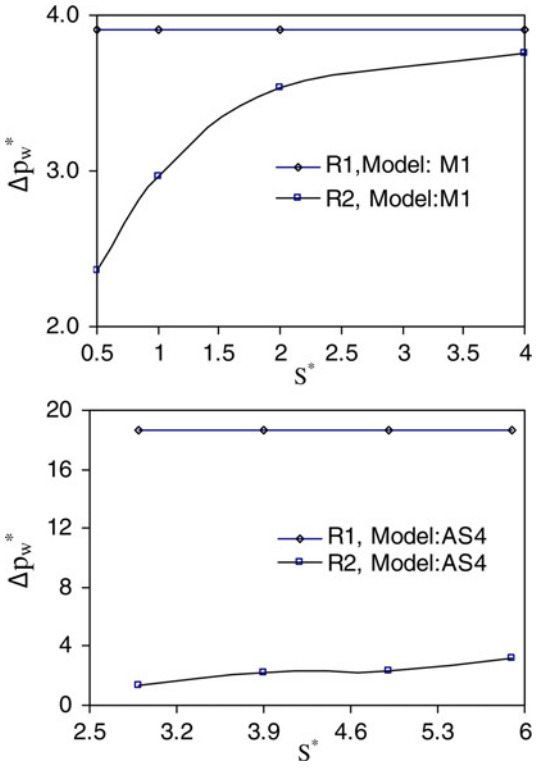

Figure 16.
Variations of wall pressure drop for Re = 100

common S*. The zone of plaque deposition is more in R_1 for all restriction spacings in comparison to R_2. No notable variation of impact has been observed at R_2 with the variation of restriction spacing. The damaging chance of arterial wall due to peak wall shear stress is also high for R_1, which remains constant for all restriction spacings in case of respective model separately. For R_2, this impact increases with increase in restriction spacing. It is also interesting to note that at R_2, the said impact is more in case of M1 than that of AS4 for the common range of S*.

3.3 Effect of Reynolds number (for model:M1 and model:AS4)

In this subsection, the simulation of flow characteristics for the models M1 with S* = 4.0, and AS4 with S* = 3.9 has been carried out for the Reynolds numbers of 100, 200, 300 and 400.

The variations of wall pressure drop at the restriction zone, variations of peak wall shear stress and streamline contour for all Reynolds numbers and for all these models of M1 and AS4 have been shown in Figures 20(a), (b) and (c). From the figure of wall pressure drop, it is noted that the magnitude of non-dimensional pressure drop decreases with the increase in Reynolds number for all considered models and for both restrictions (R1 and R2). The magnitude of ΔPw^*_2 for the model AS4 decreases with Re, but after some value of Re this value becomes zero. It may be due to merging of recirculation eddy of first restriction with the recirculating eddy of the second restriction. This is substantiated by the figure of streamline contour (Figure 20(c)). This

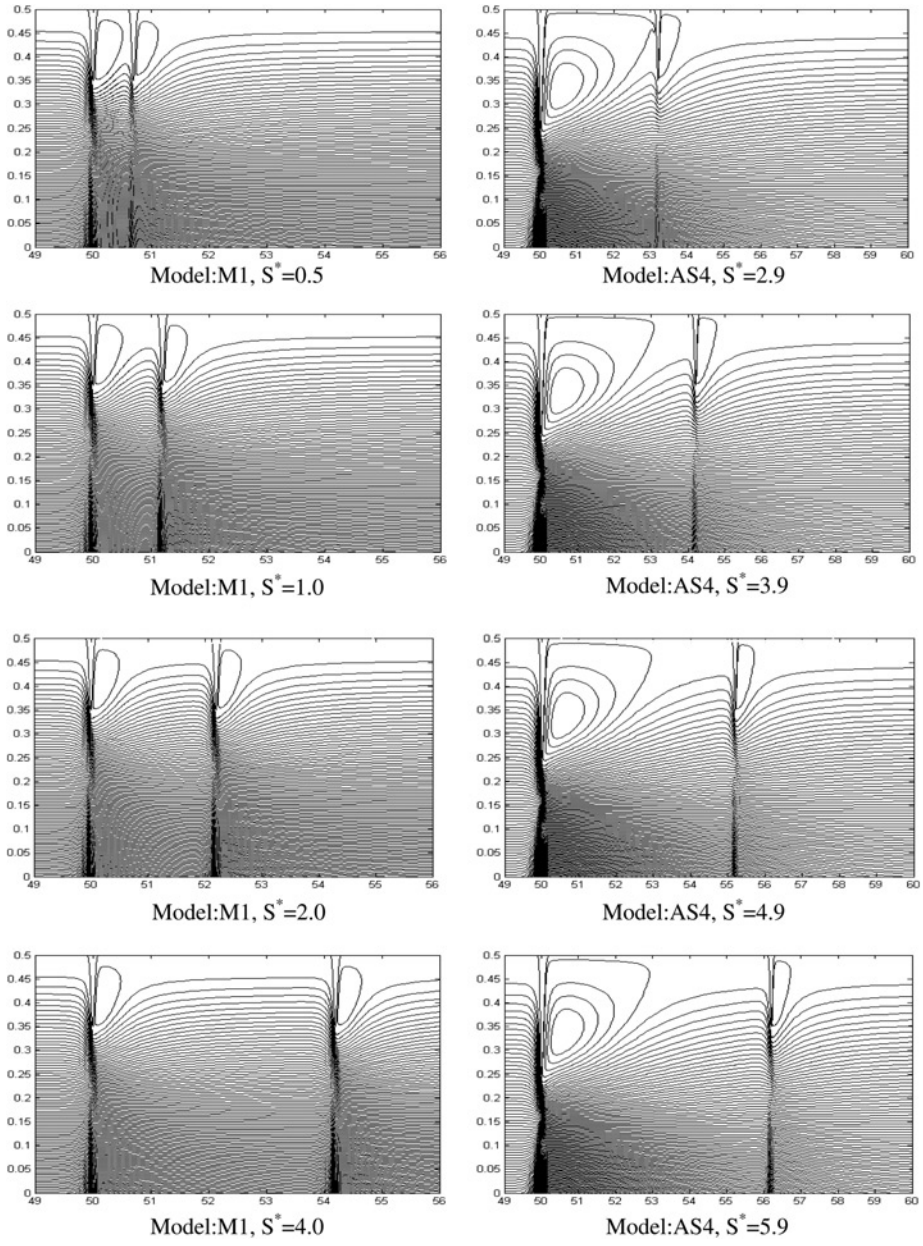

Figure 17.
Contours plotting at Re = 100

phenomenon of zero pressure drops has been observed for smaller restriction spacing also. From the figure of streamline contour, it is observed that the size of recirculation bubble for both the restrictions increases with Reynolds number for all models. From Figure 20(b), it can be mentioned that the magnitude of peak wall shear stress for both restrictions of the model:M1 increases with Reynolds number. In case of model:AS4, the

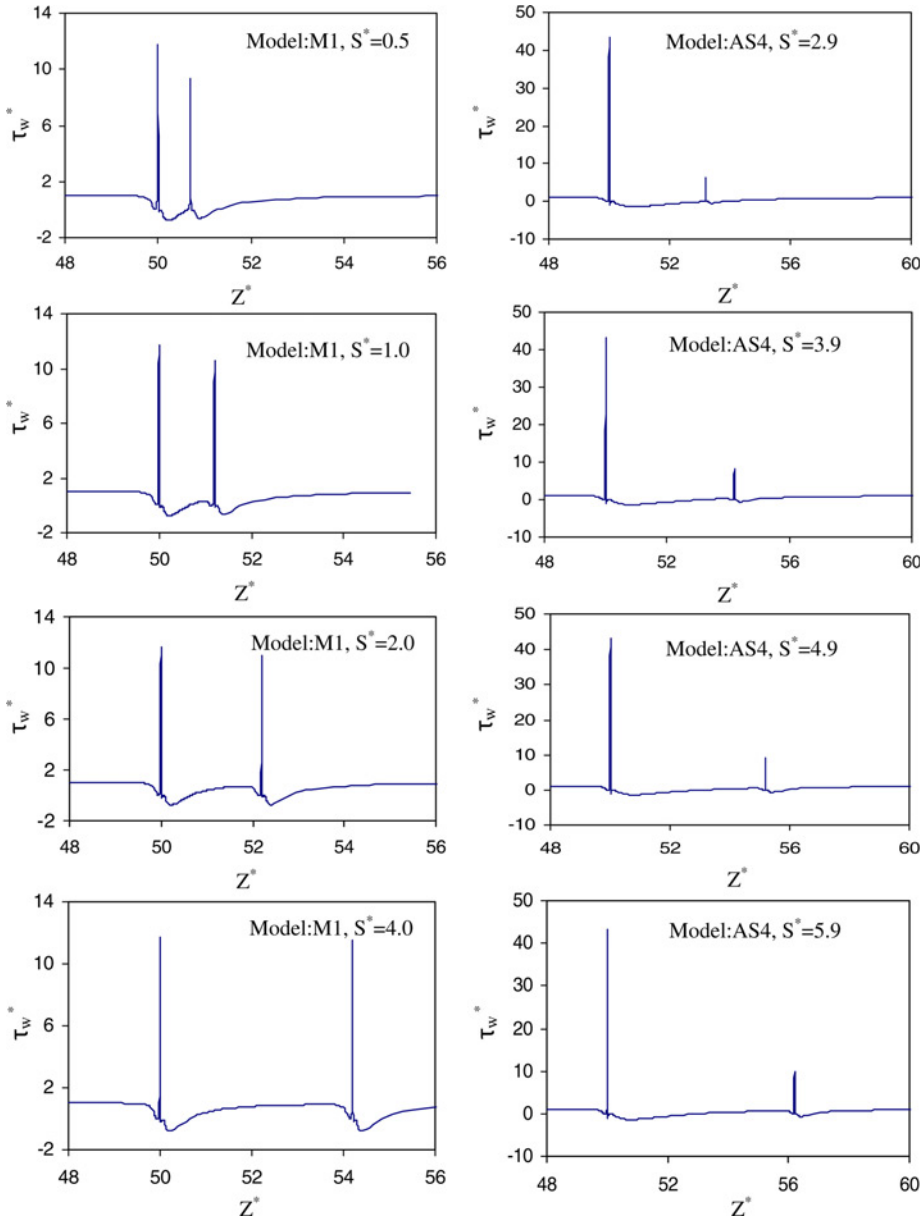

Figure 18.
Variations of wall shear stress for Re = 100

magnitude of peak wall shear stress for first restriction increases with Reynolds number, but this value decreases with Reynolds number for second restriction and attains negative peak wall shear stress value due to merging of recirculation bubble.

So, the tearing chance of arterial wall due to wall pressure and plaque deposition zone due to recirculation eddy increase with the increase in Reynolds number for both

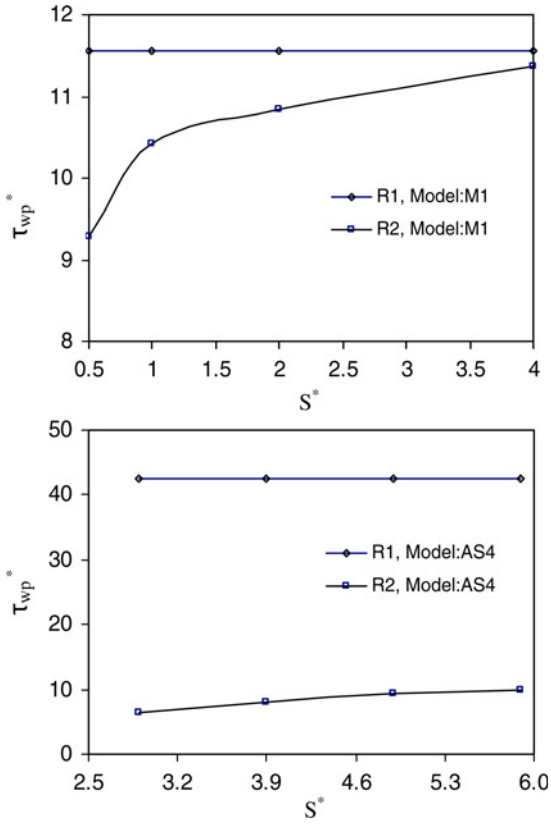

Figure 19.
Variations of peak wall stress for Re = 100

restrictions (R_1 and R_2) for models M1 and AS4. The chance of damaging of arterial wall due to peak wall shear stress increases with Reynolds number at R_1 for M1 and AS4. In case of R_2, the chance of aggravation of the disease due to peak wall shear stress for M1 increases with Re. In case of AS4, the aggravation of disease initially decreases with Re due to peak wall shear stress, but gradually the chance of aggravation of the disease due to low wall shear stress appears finally.

4. Conclusions

In the present numerical study, the effect of different shaped stenoses, restriction spacing and Reynolds number on the flow characteristics like wall pressure, streamline contour and wall shear stress of blood flow through different double bell-shaped stenosed coronary artery has been investigated and the role of all the flow characteristics on the progression of the disease, atherosclerosis, is discussed.

During our study on the effect of different shaped stenoses on flow characteristics and finally on the progression of the disease, it is revealed that the chance of tearing possibilities of arterial wall due to pressure drop at the first restriction decreases in case-1, and increases in case-2. This chance remains same at the second restriction in case-1, and decreases in case-2. The zone of plaque deposition on the artery wall due to

the length of recirculating bubble at the downstream of first restriction decreases in case-1, which increases in case-2. This zone at the downstream of the second restriction remains same in case-1; and for case-2, this zone depends upon stenosis severity of first restriction and restriction spacing. Due to peak wall shear stress, the chance of damaging in arterial wall at the first restriction decreases in case-1, and increases in case-2. This chance of damage at second restriction remains same in case-1. It decreases for case-2, and finally the impact of low wall shear stress appears.

From the outcome of numerical investigation on the impact of restriction spacing on flow characteristics and progression of the disease, it is observed that the impact of pressure drop, recirculation zone and peak wall shear stress are more at the first restriction irrespective of any value of considered restriction spacing. The quantum of impact due to pressure drop, reattachment length and peak wall shear stress remains same separately in respective cases for respective models (M1 and AS4). For second restriction, the impact due to pressure drop and peak wall shear stress increases with restriction spacing. No notable impact of recirculation zone has been observed at the second restriction for our considered case.

The impact due to pressure drop and recirculating eddy on the progression of disease increases with Reynolds number for both the restrictions for both the models, i.e., M1 and AS4. Whereas, the impact of peak wall shear stress is noted to be increasing with Reynolds number for first restriction only for both the models. In case of second restriction, as Re increases, this impact increases for model:M1 and decreases for model:AS4 with the final appearance of the effect of low wall shear stress.

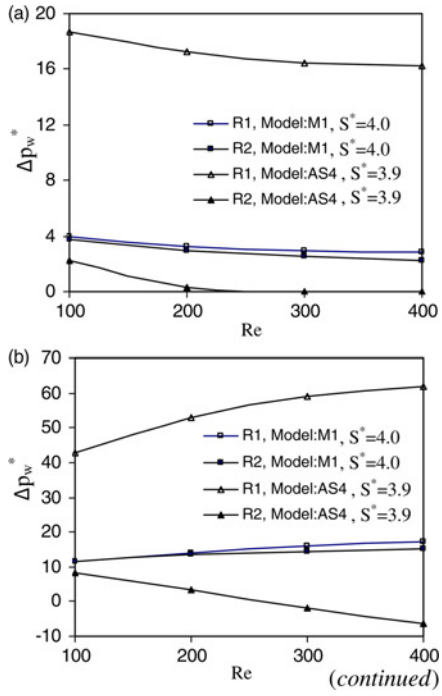

Figure 20.

(continued)

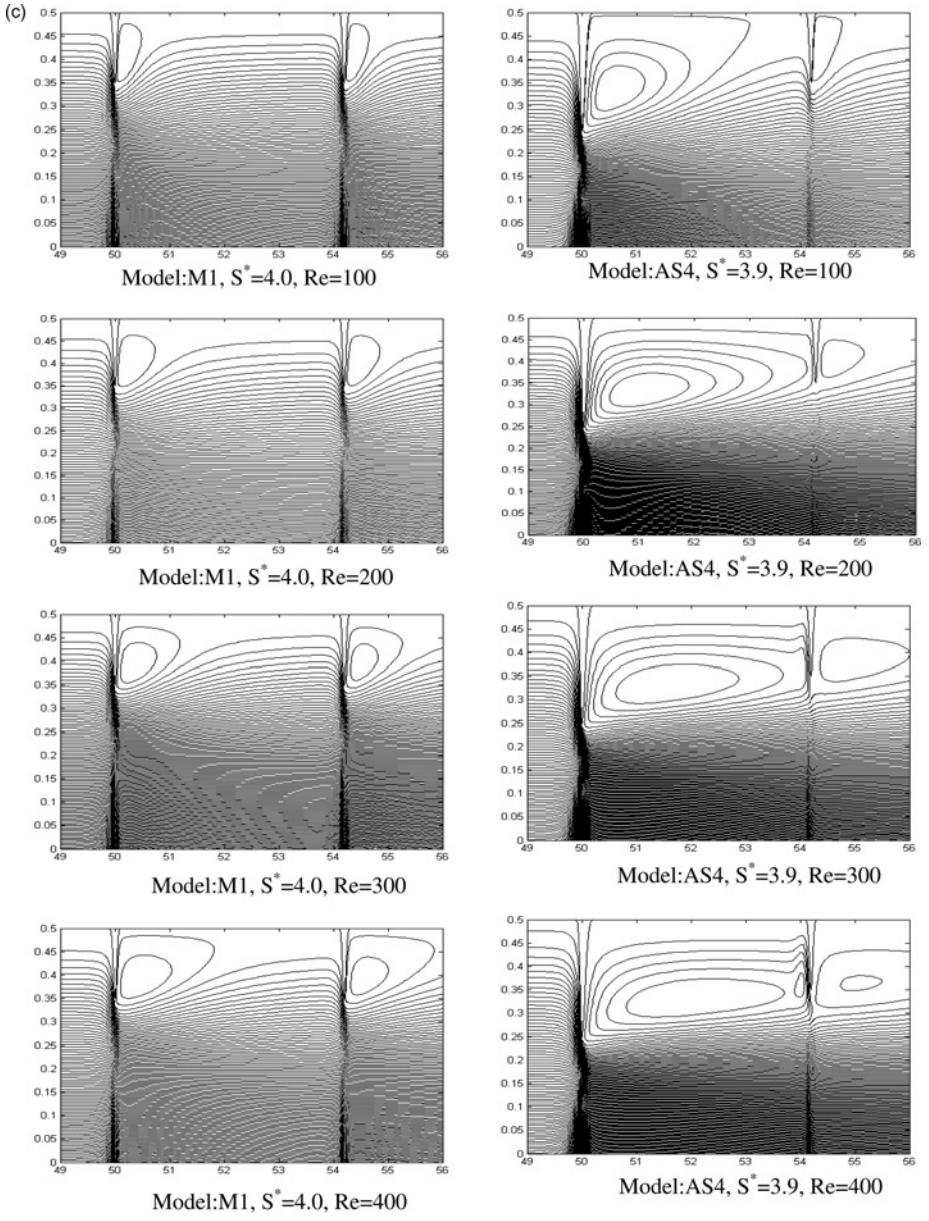

Notes: (a) Variations of wall pressure drop; (b) variations of peak wall shear stress; and (c) contours plotting

Figure 20.

Notes

1. Research Training Network on Mathematical Modelling for Haemodynamics, HaeMOdel, available at: http://iacs.epfl.ch/cmcs/Haemodel.php3

References

Ahmed, S.A. and Giddens, D.P. (1983a), "Velocity measurements in steady flow through axisymmetric stenoses at moderate Reynolds numbers", *Journal of Biomechanics*, Vol. 16 No. 7, pp. 505-16.

Ahmed, S.A. and Giddens, D.P. (1983b), "Flow disturbance measurements through a constricted tube at moderate Reynolds numbers", *Journal of Biomechanics*, Vol. 16 No. 12, pp. 955-63.

Amornsamankul, S., Wiwatanapataphee, B., Wu, Y.H. and Lenbury, Y. (2006), "Effect of non-Newtonian behaviour of blood on pulsatile flows in stenotic arteries", *International Journal of Biomedical Sciences*, Vol. 1 No. 1, pp. 306-1216.

Andersson, H.I., Halden, R. and Glomsaker, T. (2000), "Effects of surface irregularities on flow resistance in differently shaped arterial stenoses", *Journal of Biomechanics*, Vol. 33, pp. 1257-62.

Back, L.H. and Banerjee, R.K. (2000), "Estimated flow resistance increase in a spiral human coronary artery segment", *Journal of Biomechanical Engineering*, Vol. 122, pp. 675-7.

Beratlis, N., Balaras, E., Parvinian, B. and Kiger, K. (2005), "A numerical and experimental investigation of transitional pulsatile flow in a stenosed channel", *Journal of Biomechanical Engineering*, Vol. 127 No. 1, pp. 1147-57.

Bertolotti, C., Deplano, V., Fuseri, J. and Dupouy, P. (2001), "Numerical and experimental models of post-operative realistic flows in stenosed coronary bypasses", *Journal of Biomechanics*, Vol. 34, pp. 1049-64.

Buchanan Jr., J.R., Kleinstreuer, C. and Comer, J.K. (2000), "Rheological effects on pulsatile hemodynamics in a stenosed tube", *Computers & Fluids*, Vol. 29, pp. 695-724.

Chahed, N., Peronneau, P., Delouche, A. and Diebold, B. (1991), "Velocity profiles and streamlines of a revolution post-stenotic flow", *Biorheology*, Vol. 28 No. 5, pp. 383-400.

Cheng, L.C., Clark, M.E. and Robertson, J.M. (1972), "Numerical calculations of oscillating flow in the vicinity of square wall obstacles in plane conduits", *Journal of Biomechanics*, Vol. 5, pp. 467-84.

Cheng, L.C., Robertson, J.M. and Clark, M.E. (1974), "Calculation of plane pulsatile flow past wall obstacles", *Computers & Fluids*, Vol. 2, pp. 363-80.

Damodaran, V., Rankin, G.W. and Zhang, C. (1996), "Numerical study of steady laminar flow through tubes with multiple constrictions using curvilinear coordinates", *International Journal of Numerical Method in Fluids*, Vol. 23, pp. 1021-41.

Deshpande, M.D., Giddens, D.P. and Mabon, R.F. (1976), "Steady laminar flow through modelled vascular stenoses", *Journal of Biomechanics*, Vol. 9 No. 4, pp. 165-74.

Dreumel, S.C. and Kuiken, G.D.C. (1989), "Steady flow through a double converging-diverging tube model for mild coronary stenosis", *Journal of Biomechanical Engineering*, Vol. 111, pp. 212-21.

Ganong, W.F. (2001), *Review of Medical Physiology*, Appleton, New York, NY.

Griffith, M.D., Leweke, T., Thompson, M.C. and Hourigan, K. (2008), "Steady inlet flow in stenotic geometries: convective and absolute instabilities", *Journal of Fluid Mechanics*, Vol. 616, pp. 111-33.

Griffith, M.D., Leweke, T., Thompson, M.C. and Hourigan, K. (2009), "Pulsatile flow in stenotic geometries: flow behaviour and stability", *Journal of Fluid Mechanics*, Vol. 622, pp. 291-320.

Hasan, A.B.M. and Das, D.K. (2008), "Numerical simulation of sinusoidal fluctuated pulsatile laminar flow through stenotic artery", *Journal of Applied Fluid Mechanics*, Vol. 1 No. 2, pp. 25-35.

Jung, H., Choi, J.W. and Park, C.G. (2004), "Asymmetric flows of non-Newtonian fluids in symmetrical stenosed artery", *Korea-Australia Rheology*, Vol. 16 No. 2, pp. 101-8.

Layek, G.C., Mukhopadhyay, S. and Gorla, R.S.R., (2009), "Unsteady viscous flow with variable viscosity in a vascular tube with an overlapping constriction", *International Journal of Engineering Science*, Vol. 47, pp. 649-59.

Lee, J.S. and Fung, Y.C. (1970), "Flow in locally constricted tubes at low Reynolds number", *Journal of Applied Mechanics*, Vol. 37, pp. 9-16.

Lee, K.W. and Xu, X.Y. (2002), "Modelling of flow and wall behaviour in a mildly stenosed tube", *Medical Engineering & Physics*, Vol. 24, pp. 575-86.

Lee, T.S. (1994), "Steady laminar fluid flow through variable constrictions in vascular tube", *Journal of Fluid Engineering*, Vol. 116, pp. 258-89.

Lee, T.S. (2002), "Numerical study of fluid flow through double bell-shaped constrictions in a tube", *International Journal of Numerical Methods for Heat and Fluid Flow*, Vol. 12 No. 3, pp. 258-89.

Lee, T.S. (2005), "Numerical studies of fluid flow through tubes with double constrictions", *International Journal of Numerical Methods in Fluids*, Vol. 11 No. 8, pp. 1113-26.

Liao, W., Lee, T.S. and Low, H.T. (2004), "Numerical studies of physiological pulsatile flow through constricted tube", *International Journal of Numerical Methods for Heat & Fluid Flow*, Vol. 14 No. 5, pp. 689-713.

Liepsch, D., Singh, M. and Lee, M. (1992), "Experimental analysis of the influence of stenotic geometry on steady flow", *Biorheology*, Vol. 29 No. 4, pp. 419-31.

Liu, G.-T., Wang, X.-J., Ai, B.-Q. and Liu, L.-G. (2004), "Numerical study of pulsating flow through a tapered artery with stenosis", *Chinese Journal of Physics*, Vol. 42 No. 4-I, pp. 401-9.

Mallinger, F. and Drikakis, D. (2002), "Instability in three-dimensional, unsteady, stenotic flows", *International Journal of Heat and Fluid Flow*, Vol. 23, pp. 657-63.

Mandal, D.K. and Chakrabarti, S. (2007), "Study of pressure drop and flow characteristics across rectangular stenotic models", *International Journal for Fluid Mechanics Research*, Vol. 34 No. 5, pp. 434-61.

Mandal, D.K. and Chakrabarti, S. (2008), "Effect of stricture length on reattachment point and wall shear stress through a stenosed coronary artery", *International Journal for Fluid Mechanics Research*, Vol. 35 No. 2, pp. 188-202.

Mates, R.E., Gupta, R.L., Bell, A.C. and Klocke, F.J. (1978), "Fluid dynamics of coronary artery stenosis", *Circulation Research*, Vol. 42, pp. 152-62.

Misra, J.C. and Shit, G.C. (2006), "Blood flow through arteries in a pathological state: a theoretical study", *International Journal of Engineering Science*, Vol. 44, pp. 662-71.

Mittal, R., Simmons, S.P. and Najjar, F. (2003), "Numerical study of pulsatile flow in a constricted channel", *Journal of Fluid Mechanics*, Vol. 485, pp. 337-78.

Moore, K.L. (1990), *Clinically Oriented Anatomy*, Williams and Wilkins, Baltimore, MD.

Neofytou, P. and Drikakis, D. (2003), "Effects of blood models on flows through a stenosis", *International Journal of Numerical Methods in Fluids*, Vol. 43, pp. 597-635.

Ojha, M., Cobbold, C., Johnston, K.W. and Hummel, R.L. (1989), "Pulsatile flow through constricted tubes: an experimental investigation using photochromic tracer methods", *Journal of Fluid Mechanics*, Vol. 203, pp. 173-97.

Patankar, S.V. (1980), *Numerical Heat Transfer*, North Holland, New York, NY.

Pincombe, B. and Mazumdar, J. (1997), "The effects of post-stenotic dilatations on the flow of a blood analogue through stenosed coronary arteries", *Mathematical and Computer Modelling*, Vol. 25 No. 6, pp. 57-70.

Pontrelli, G. (2001), "Blood flow through an axisymmetric stenosis", *Proceedings of the Institution Of Mechanical Engineers, Part-H, Journal of Engineering in Medicine*, Vol. 215 No. 1, pp. 1-10.

Ramaswamy, S.D., Vigmostad, S.C., Wahle, A., Lai, Y.-G., Olszewski, M.E., Braddy, K.C., Brennan, T.M.H., Rossen, J.D., Sonka, M. and Chandran, K.B. (2004), "Fluid dynamic analysis in a

human left anterior descending coronary artery with arterial motion", *Annals of Biomedical Engineering*, Vol. 32 No. 12, pp. 1628-41.

Ramaswamy, S.D., Vigmostad, S.C., Wahle, A., Lai, Y.-G., Olszewski, M.E., Braddy, K.C., Brennan, T.M.H., Rossen, J.D., Sonka, M. and Chandran, K.B. (2006), "Comparison of left anterior descending coronary artery hemodynamics before and after angioplasty", *Journal of Biomechanical Engineering*, Vol. 128, pp. 40-8.

Rathish Kumar, B.V., Yamaguchi, T., Liu, H. and Himeno, R. (2002), "A numerical study of an unsteady laminar flow in a doubly constricted 3D vessel", *International Journal of Numerical Methods in Fluids*, Vol. 38, pp. 1159-76.

Sankar, D.S. and Lee, U. (2009), "Mathematical modeling of pulsatile flow of non-Newtonian fluid in stenosed arteries", *Communications in Nonlinear Science and Numerical Simulation*, Vol. 14, pp. 2971-81.

Seeley, B.D. and Young, D.F. (1976), "Effect of geometry on pressure losses across models of arterial stenoses", *Journal of Biomechanics*, Vol. 32, pp. 439-48.

Sherwin, S.J. and Blackburn, H.M. (2005), "Three-dimensional instabilities and transition of steady and pulsatile axisymmetric stenotic flows", *Journal of Fluid Mechanics*, Vol. 533, pp. 297-327.

Siouffi, M., Deplano, V. and Pelissier, R. (1998), "Experimental analysis of unsteady flows through a stenosis", *Journal of Biomechanics*, Vol. 31, pp. 11-19.

Solzbach, U., Wollschlager, H., Zeiher, A. and Just, H. (1987), "Effect of stenotic geometry on flow behaviour across stenotic models", *Medical and Biological Engineering and Computing*, Vol. 25, pp. 543-50.

Tandom, P.N., Rana, U.V.S., Kawahara, M. and Katiyar, V.K. (1993), "A model for blood flow through a stenotic tube", *International Journal of Biomedical Computing*, Vol. 32, pp. 61-78.

Tu, C. and Deville, M. (1996), "Pulsatile flow of non-Newtonian fluids through arterial stenoses", *Journal of Biomechanics*, Vol. 29 No. 7, pp. 899-908.

Tu, C., Deville, M., Dheur, L. and Vanderschuren, L. (1992), "Finite element simulation of pulsatile flow through arterial stenosis", *Journal of Biomechanics*, Vol. 25 No. 10, pp. 1141-52.

Varghese, S.S. and Frankel, S.H. (2003), "Numerical modeling of pulsatile turbulent flow in stenotic vessels", *Journal of Biomechanical Engineering*, Vol. 125, pp. 445-60.

Young, D.F. and Tsai, F.Y. (1973a), "Flow characteristics in models of arterial stenoses-I: steady flow", *Journal of Biomechanics*, Vol. 6 No. 4, pp. 395-410.

Young, D.F. and Tsai, F.Y. (1973b), "Flow characteristics in models of arterial Stenoses-II: unsteady flow", *Journal of Biomechanics*, Vol. 6 No. 5, pp. 547-59.

Zendehbudi, G.R. and Moayeri, M.S. (1999), "Comparison of physiological and simple pulsatile flows through stenosed arteries", *Journal of Biomechanics*, Vol. 32, pp. 959-69.

Corresponding author
S. Chakrabarti can be contacted at: somnathbec@rediffmail.com